Optics and Laser Technology 108 (2018) 235–240

Contents lists available at ScienceDirect

Optics and Laser Technology

journal homepage: www.elsevier.com/locate/optlastec

Full length article

Attosecond control of correlated electron dynamics in strong-field nonsequential double ionization by parallel two-color pulses

Xiaomeng Ma[a], Yueming Zhou[a,*], Ning Li[a], Min Li[a], Peixiang Lu[b]

[a] School of Physics and Wuhan National Laboratory for Optoelectronics, Huazhong University of Science and Technology, Wuhan 430074, PR China
[b] Laboratory of Optical Information Technology, Wuhan Institute of Technology, Wuhan 430205, PR China

ARTICLE INFO

Article history:
Received 29 November 2017
Received in revised form 15 May 2018
Accepted 24 June 2018

2010 MSC:
00-01
99-00

Keywords:
Multiphoton process
Ionization
Strong-field process

ABSTRACT

We theoretically investigate the correlated electron dynamics in strong-field nonsequential double ionization (NSDI) of Ar by the parallel two-color pulses consisting of 800- and 400-nm laser fields with the semiclassical ensemble model. Our calculations show that the momentum distributions of Ar^{2+} in the direction parallel to the polarization of laser field exhibit the single- or double-hump structure, depending on the relative phase of the two-color fields. Back analysis of the NSDI trajectories reveals that recollision of returning electron is well confined in a time window of several attoseconds, and the position of which can be controlled with attosecond precision by changing the relative phase of the two-color fields. Thus, the recollision energy is accurately controlled with the two-color fields. As a consequence, the time delay between the double ionization and recollision changes with the relative phase, resulting in the relative-phase-dependent ion momentum distributions. More interestingly, the different peaks of ion momentum spectra result from the NSDI events with different time delays between double ionization and recollision. Thus, the corresponding correlated electron dynamics for different peaks in the ion momentum distributions can be directly determined in the two-color fields.

1. Introduction

Tunneling of atoms or molecules in strong laser field usually is accompanied by recollision, where the tunneling electron is accelerated in the laser field and then returns back to the parent ion when the electric field of the driving laser pulse changes its direction [1,2]. This recollision leads to various interesting phenomena, such as high harmonic generation (HHG) [3–5], high-energy above-threshold ionization (HATI) [6–10], and nonsequential double ionization (NSDI) [11–14]. Among these phenomena, NSDI has attracted special attention due to the highly correlated behavior of the ionized electron pairs during the inelastic recollision [15]. In past decades, a great number of experimental [16–20] as well as theoretical studies [21–32] have been performed to explore the correlated dynamics of the electron pairs in NSDI.

Previous studies have shown that the correlated electron dynamics in NSDI is rather complicated and sensitively depends on the driving laser pulses. Generally, NSDI could occur through two different pathways, recollision impact ionization (RII) and recollision-excitation with subsequent field ionization (RESI) [33]. At low laser intensities where the maximum recollision energy of the first electron is not enough to ionize the second electron directly, NSDI occurs through the RESI pathway. At high laser intensities, the recollision energy of the first electron is higher than the ionization potential of the second electron and thus double ionization can occur through the RII pathway. Usually, in the NSDI experiments the recollision energy of the returning electron spans over a wide range and thus both RII and RESI pathways make contribution, complicating the analysis of the dynamics in NSDI. Additionally, in the multi-cycle laser pulses, the multiple-recollision process also contributes to NSDI [34,35]. Moreover, the multiple-returning-recollision process, where recollision occurs at the later other than the first returning of the tunneled electron, has significant contribution to the total NSDI yields, especially in the mid-infrared laser fields [36–38]. The combined contribution of these processes hampers a full exploration of the detailed microscopic dynamics in NSDI. Revealing and ultimately controlling the correlated electron dynamics are the central tasks in current studies on strong-field NSDI.

With the development of the laser technology, ultrashort few-cycle laser pulses with stabilized carrier-envelope phase are widely available in laboratory [39]. In few-cycle pulses, the multiple-recollision and multiple-returning-recollision processes are

* Corresponding author.
E-mail address: zhouymhust@hust.edu.cn (Y. Zhou).

https://doi.org/10.1016/j.optlastec.2018.06.058

strongly suppressed and the recollision are well confined in single optical cycle [40]. Thus the few-cycle pulses enable one to study the microscopic electron dynamics of NSDI in a much more clean way [41]. Additionally, in the multi-cycle pulses, there are considerable NSDI events occurring through the RESI pathway with a time delay longer than one optical cycle between double ionization and recollision [42,43]. While in the few-cycle pulses, this time delay is well within one optical cycle. Thus, the subcycle electron dynamics can be revealed with the few-cycle pulses. Taking these advantages of the few-cycle pulses, for example, the decay dynamics of the doubly excited state formed by recollision in NSDI is unambiguously traced [44]. The subcycle ionization dynamics of RESI in the few-cycle is clearly visualized and the asymmetric energy sharing during recollision is also revealed [41]. Moreover, the few-cycle pulse provides a feasible way to control NSDI. It has been reported that the ion momentum distributions as well as the correlated electron momentum spectra can be manipulated by changing the carrier-envelope phase of the few-cycle pulses and more details of the correlated electron dynamics have been uncovered [40,45]. Recently, control of NSDI with the few-cycle pulses has draw extensive attentions.

The two-color laser pulse is another powerful tool in controlling the recollision processes in strong laser fields [46,47]. Compared with the few-cycle pulses, it has more parameters for control, for example, the relative phase, relative intensity, polarizations et al. The scheme of two-color pulses has been widely employed to control the electron dynamics in HHG and ATI [48,49]. Recently, the two-color field has also been used to control the electron correlations in strong-field NSDI [50]. For example, with the orthogonal two-color pulses, the electron pairs can be controlled to exhibit correlated or anticorrelated behaviors [51]. With the circularly polarized two-color laser pulses, the double ionization yields have been manipulated by adjusting the relative intensity ratio of the two fields [52,53]. In this paper, using a semiclassical ensemble model, we theoretically study the correlated electron dynamics in the parallel two-color fields consisting of an 800-nm and a 400-nm laser pulses. We focus on the RESI pathway of NSDI. Our results show that the subcycle decay process of the excited states induced by recollision in RESI pathway can be controlled by changing the relative phase of the two-color fields. Back analysis of the NSDI trajectories shows that this is based on the attosecond control of the recollision time and thus the recollision energy of the tunneled electron. The controlling of the subcycle decay process results in the relative phase dependence of the experimentally observable ion momentum distributions. Interestingly, in the ion momentum distributions, different peaks originate from the NSDI events with different time delays between double ionization and recollision. Thus, the correlated electron dynamics of NSDI can be directly judged from the observable ion momentum distributions.

2. Method

Accurately describing NSDI in strong laser fields needs numerically solving the time-dependent Schrödinger equation. However, for the two- and multi-electron systems, the computational demand of this method is huge [21,54,55]. In the past decades numerous studies have resorted to the classical and semiclassical models, which have been very successful in explaining various phenomena in NSDI, for example, the V-like [27,56,57] and cross-like structures [41,58] in the correlated electron momentum spectra, and the anticorrelation of the electron pairs in low laser intensities [59]. The (semi) classical models are also successful in predicting phenomena in strong-field NSDI [51,60,61]. Moreover, with the (semi) classical model, the electron dynamics in NSDI can be intuitively revealed by back tracing the NSDI trajectories [29,62,63]. Therefore, here we employ the semiclassical ensemble model [27,64] to investigate the correlated electron dynamics of NSDI by the parallel two-color pulses. In the semiclassical model, the first electron is ionized through tunneling with the rate given by tunneling theory [65]. The subsequent evolutions of the tunneled and the bound electrons are described by the Newton's classical motion equation (atomic units are used throughout until stated otherwise):

$$\frac{d^2\mathbf{r}_i}{dt^2} = -\nabla[V_{ne}(\mathbf{r}_i) + V_{ee}(\mathbf{r}_1,\mathbf{r}_2)] - \mathbf{E}(t), \tag{1}$$

where the indicates $i = 1$, 2 refer to the first and the second electrons, respectively. $V_{ne}(\mathbf{r}_i) = -2/\sqrt{\mathbf{r}_i^2 + a^2}$ and $V_{ee}(\mathbf{r}_1,\mathbf{r}_2) = 1/\sqrt{(\mathbf{r}_1-\mathbf{r}_2)^2 + b^2}$ represent the ion-electron and electron-electron coulomb interaction potentials, respectively. A soft parameter a is employed to avoid autoionization of the two-electron system [56]. Here we set a =1.5. The parameter b in the electron-electron interaction potential is not important as long as it is small enough. Here we set b =0.01. The electric field of the parallel two-color pulse is written as $\mathbf{E}(t) = f(t)[\mathrm{E}_0\cos(\omega t)\hat{\mathbf{x}} + \sqrt{\varepsilon}\mathrm{E}_0\cos(2\omega t + \Delta\phi)\hat{\mathbf{x}}]$, where the pulse envelope $f(t)$ has a constant amplitude for the first eight cycles and is linearly turned off with a two-cycle ramp. E_0 is the amplitude of the 800-nm field and ε is the intensity ratio of the 800-nm and 400-nm fields. $\Delta\phi$ is the relative phase between the 400-nm and 800-nm fields. ω is the frequency of the 800-nm laser field.

The initial conditions of the two electrons for Eq. (1) are obtained as follows. The first tunneling electron has zero parallel (with respect to the direction of electric field) velocity and a Gaussian-like transverse velocity distribution. The weight of each trajectory is $w(t_0, \upsilon_{\perp 0}) = w(t_0)w(\upsilon_{\perp 0})$ [64], in which

$$w(t_0) = \left[\frac{2(2\mathrm{I}_{p1})^{1/2}}{|\mathbf{E}(t_0)|}\right]^{\frac{2}{\sqrt{2\mathrm{I}_{p1}}}-1} \exp\left[\frac{-2(2\mathrm{I}_{p1})^{3/2}}{3|\mathbf{E}(t_0)|}\right], \tag{2}$$

$$w(\upsilon_{\perp 0}) = \frac{1}{|\mathbf{E}(t_0)|}\exp\left[-\frac{\upsilon_{\perp 0}^2(2\mathrm{I}_{p1})^{1/2}}{|\mathbf{E}(t_0)|}\right], \tag{3}$$

where $w(t_0)$ is the instantaneous tunneling probability and $w(\upsilon_{\perp 0})$ is the distribution of the initial transverse momentum $\upsilon_{\perp 0}$ of the first electron. For the second electron, the initial position and momentum are depicted by microcanonical distribution of ground state energy of Ar^+. In our calculations, the first and second ionization potentials are chosen as $\mathrm{I}_{p1} = 0.58$ a.u. and $\mathrm{I}_p2 = 1.01$ a.u., respectively, to match those of Ar. Several millions weighted classical two-electron trajectories are traced from the tunneling moment t_0 to the end of the pulse. The double ionization events are determined if the energies of both electrons are positive after the laser field is turned off.

3. Results and discussions

We first show the ratio of Ar^{2+}: Ar^+ as a function of the relative phase in Fig. 1(a). Here we consider three cases: $I_{800} = 1.0\times10^{14}$ W/cm^2 with the intensity ratio $\varepsilon = 0.1$ (i), $\varepsilon = 0.2$ (ii) and $I_{800} = 0.6\times10^{14}$ W/cm^2 with $\varepsilon = 0.1$ (iii). It shows that the ratio of Ar^{2+}: Ar^+ exhibits an oscillating behavior with a period of π and this behavior is similar for these three cases. It indicates that NSDI has indeed been controlled by the linear two-color laser fields. More information of the two-electron dynamics can be obtained from the momentum distribution. In Fig. 1(b)–(d), we show the momentum distributions of the ion along the laser polarization direction as a function of the relative phase. In Fig. 1(b), the

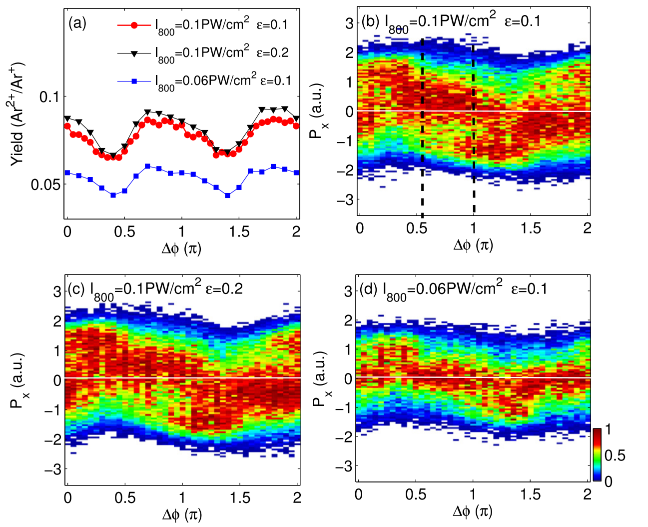

Fig. 1. (a) The ratio of Ar^{2+}: Ar^{+} as a function of the relative phase. (b)–(d) The momentum distribution of Ar^{2+} in the parallel direction (parallel to the laser polarization) as a function of the relative phase. The white transverse lines indicate zero momentum and are added to guide the eyes. The dashed vertical lines in (b) denote the cases of $\Delta\phi = 0.55\pi$ and 1.1π, respectively, which are detailedly analyzed in the text. The distributions are normalized at each phase. The laser intensities of the 800-nm fields and the intensity ratios are labeled in the figure.

distribution oscillates with the relative phase. For $\Delta\phi = 0$, the distribution is mainly located in $P_{xion} > 0$, and it gradually moves to $P_{xion} < 0$ as $\Delta\phi$ increases and then moves to $P_{xion} > 0$ again. Close inspection shows that the distribution exhibits a double-hump or single-hump structure, depending on the relative phase. The distributions shown in Fig. 1(c) and (d) exhibit similar behaviors except that in Fig. 1(d) the distribution always exhibits the single-hump structure.

In order to reveal the corresponding dynamics of electrons in the two-color fields, we back trace the classical trajectories and perform statistical analysis [29,57]. We take the case in Fig. 1(b) as an example. Fig. 2(a)–(c) show the distributions of tunneling

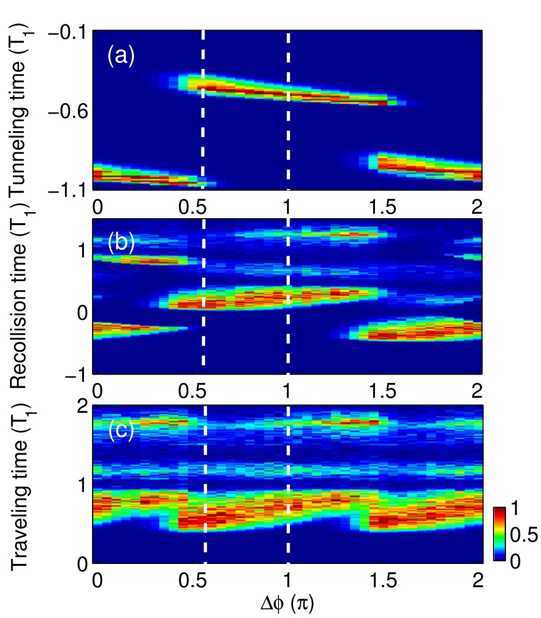

Fig. 2. Distributions of the tunneling time (a), recolllsion time (b), the traveling time (c) as a function of the relative phase for the NSDI events. The distributions are normalized at each phase.

time, the recolllsion time, and the traveling time for the NSDI events as a function of the relative phase, respectively. Here the recollision is defined when this distance is less than 3.0 a.u. after the tunneling of the first electron and the recollision time is defined as the instant of closest approach of the two electrons. In our calculations, for almost all of the double ionization events, the closest distance is less than 3 a.u., meaning that double ionization occur through the recollision. We have checked that a small change of this criterion does not change the final results. The traveling time is the time difference between recollision and tunneling of the first electron, and the double ionization time is defined as the instant when both electrons achieve positive energies [57–59]. Note that here we only consider the NSDI events where tunneling of the first electron occurs within the optical cycle of $-1.1T_1$ to $-0.1T_1$ (T_1 is the laser cycle of the 800-nm field). For $\Delta\phi$ changing from 0.35π to 0.65π and 1.35π to 1.65π, there are two asymmetric time windows for tunneling ionization of the first electrons, while at other phases there is only one window. More interestingly, the positions of these windows change gradually with the relative phases. For example, the window locating around $-0.5T_1$ moves from $-0.4T_1$ to $-0.55T_1$ as $\Delta\phi$ changes from 0.5π to 1.5π. It means that the tunneling time of first electron has been controlled with attosecond accuracy by the two-color pulses. The recollision is directly related to the tunneling moment, and thus attosecond control of the recollision in NSDI is realized, as shown in Fig. 2(b). In Fig. 2(b), the population locating around $-0.25T_1$ and $0.25T_1$ corresponds to the events where tunneling of the first electron occurs within the time window around $-1.0T_1$ and $-0.5T_1$, respectively. The other population is resulted from the NSDI events where recollision occurs at the second and third returnings of the first electron [6,38]. This is more clearly seen in traveling time distribution shown in Fig. 2(c). For most of the events, recollision occurs at the first returning and the corresponding travelling time is less than one optical cycle. For the first-returning recollision event, the travelling time increases from $0.5T_1$ to $0.85T_1$ as the relative phase changes from 0.5π to 1.5π, indicating the attosecond control of the recollision by the two-color fields. There are also considerable events with traveling time of about 1.75 cycle which correspond to the events where recollision occurs at the third returning. The event of second-returning recollision (with the travelling time of about $1.25T_1$) is strongly suppressed in our case. This is due to the fact that the second returning possesses the lowest energy and thus it cannot lead to NSDI for the laser intensities of our calculations [6].

The control of recollision time results in the oscillating of the recollision energy with the relative phase, as shown in Fig. 3(a). The recollision energy reaches a maximal value of 0.9 a.u. at $\Delta\phi = 0.4\pi$ and 1.4π, and a minimum of 0.5 a.u at $\Delta\phi = 0.7$ and 1.7π. In NSDI, the electron dynamics after recollision critically depends on the recollision energy [33]. It can be expected that the electron dynamics after recollision can be controlled by changing the relative phase of the two-color fields. Note that for the laser parameters in our calculations, the recollision energy is always less than the ionization potential of the second electron. Fig. 3(b) displays the time delay between double ionization and recollision. It is shown that for most of the events the time delay between recollision and the ionization of the second electron is about $0.15T_1$, indicating that RESI is the dominant pathway. Interestingly, this time delay distribution depends on the relative phase. For $\Delta\phi$ around 0.7π and 1.7π, where the recollision energy is the lowest, there are significant events ionized with time delay longer than $0.25T_1$, while for other relative phases, most double ionization events occur with time delay less than $0.25T_1$. This is easy to understand. For the lower recollision energy, the second electron was excited to lower excited states and thus the subsequent ionization rate is smaller, leading to the longer time delay.

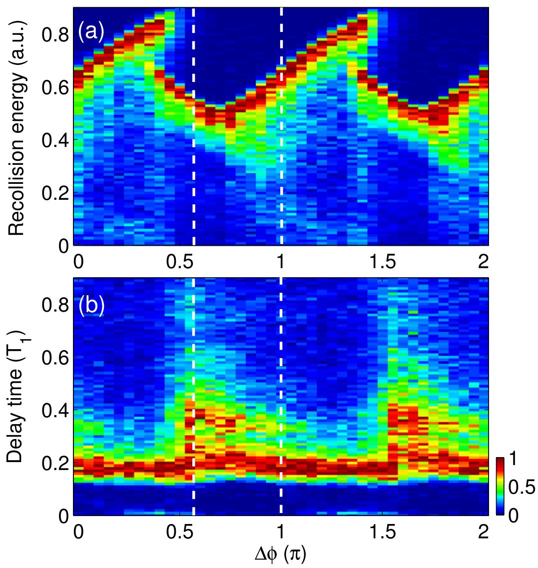

Fig. 3. Distributions of the recollision energy (a), and the time delay between double ionization and recollision (b) as a function of the relative phase. The distributions are normalized at each phase.

With the analysis above in mind, the relative phase dependence of the ion momentum distributions can be explained. We take two phases $\Delta\phi = 0.55\pi$ and 1.0π for example (indicated by the dashed lines in Fig. 1(b), Figs. 2 and 3). Fig. 4(a)–(d) show the correlated electron momentum distributions. Here we have classified the NSDI events based on the time delay between double ionization and recollision [58,59]. Fig. 4(a) and (b) shows the NSDI events where the time delay is less than $0.25T_1$. Though NSDI occurs through the RESI pathway, the correlated momentum distributions locate in the first and third quadrants for this short time delay. This has been experimentally observed and explained in the few-cycle pulses [41]. The faint repulsion behavior with respect to the main diagonal indicates the time delay between the ionization of the two electrons and their final-state coulomb repulsion [44,58,66]. For this type of NSDI event, the ion momentum distribution exhibits a double-hump structure at $\Delta\phi = 0.55\pi$, as shown by the red curve in Fig. 4(e). For $\Delta\phi = 1.0\pi$, there is only one tunneling window for the tunneling of the first electron [Fig. 2(a)], and thus only one peak appears in the ion momentum distribution, as shown in Fig. 4(f).

For the events with time delay larger than $0.25T_1$, the distributions of the correlated electron momentum are clustered near the origin and spread to the second and fourth quadrants, as shown in Fig. 4(c) and (d). Thus the corresponding ion momentum distributions exhibit the single-hump structure located around zero momentum, as shown by the blue curves in Fig. 4(e) and (f). At $\Delta\phi = 0.55\pi$, the type of events dominant NSDI, and thus the total ion momentum distribution exhibits the single-hump structure located near zero momentum, as shown by the black curve in Fig. 4(e). At $\Delta\phi = 1.0\pi$, the events with time delay larger than $0.25T_1$ is relatively fewer, and the peak at nonzero momentum is still visible in the total ion momentum distribution. Consequently, the distribution exhibits the double-hump structure. Simply speaking, the single- and double-hump structures imply the time delay between double ionization and recollision in the RESI pathway. The single-hump structure means that NSDI dominates by the RESI with time delay longer than $0.25T_1$. In the double-hump structure, the peak near zero momentum corresponds to this type of NSDI events with long time delay, and the peak located at nonzero momentum results from those events where the time delay is less than $0.25T_1$. Thus, from the experimentally observable ion momentum distributions, one can determine the corresponding electron dynamics of NSDI for the different peaks. As shown in Fig. 1(b)–(d), the peak near or around zero momentum alway has the dominant contribution to the total NSDI yields. This indicates that the RESI with time delay longer than $0.25T_1$ is prevalent, meaning the excited electron can resist ionization in the first peak of the electric field after recollision. Previous experiment has shown that the electron momentum distribution depends sensitively on the pulse duration [42]. This study shows that the events with time delay larger than $0.25T_1$ and even longer take a great part of the double ionization yields, and thus can explain the pulse-duration dependence of the electron momentum distribution.

This time delay determines the correlation patterns in the final electron momentum distributions, as shown in Fig. 4(a)–(d). We finally display the ratio of correlated and the anticorrelated emissions in the two-color fields in Fig. 5. Here the correlated and anticorrelated emissions mean that the two electrons emit into the same or opposite hemispheres, respectively. For the cases of higher laser intensities, the ratios oscillate with the relative phase and are

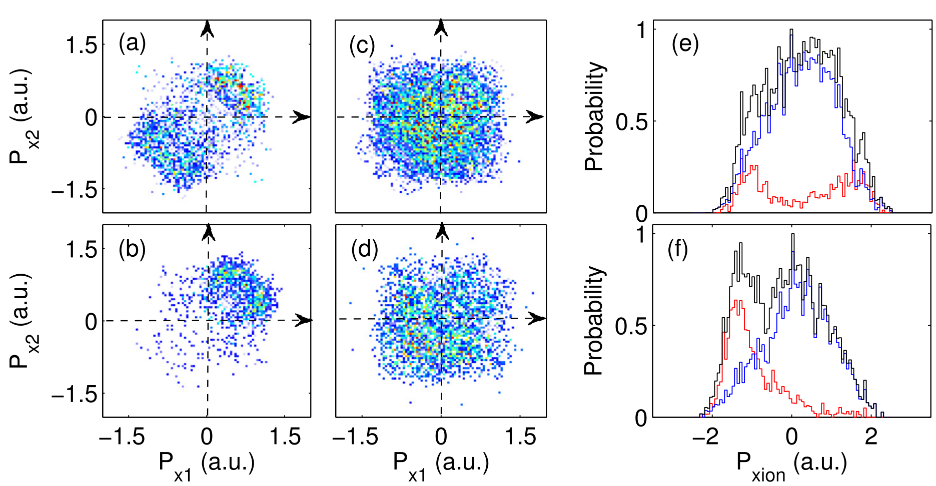

Fig. 4. Correlated electron momentum distributions along the laser polarization direction by the parallel two-color laser pules for $\Delta\phi = 0.55\pi$ (a, c) and 1.0π (b, d), respectively. (a, b) The distributions show the events with time delay less than 0.25 T_1. (c, d) The distributions show the events with time delay larger than $0.25T_1$. (e, f) The momentum distributions of Ar^{2+} for $\Delta\phi = 0.55\pi$ and 1.0π, respectively. The red curves present distributions correspond to the events with time delay less than $0.25T_1$. The blue curves present distributions correspond to the events with time delay larger than $0.25T_1$. The black curves present distributions correspond to all the events. (For interpretation of the references to color in this figure legend, the reader is referred to the web version of this article.)

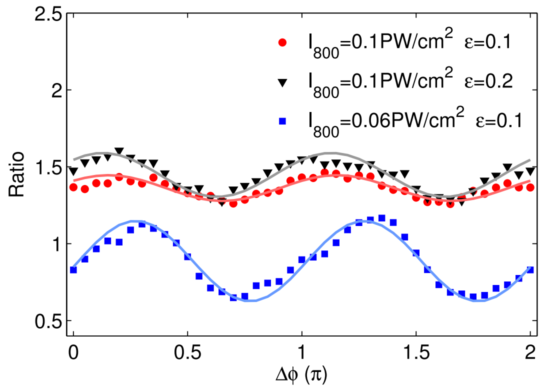

Fig. 5. The ratio of the correlated and anticorrelated emission as a function of the relative phase. The solid curves represent the corresponding fitted results with the cosine function, which are added for a better view on the oscillation of ratio. Here correlated and anticorrelated emission mean the electron pairs emitted into the same or opposite hemispheres, respectively.

alway larger than one. For the lower laser intensity the ratio oscillates around one, indicating that the electron pairs can be dominated by the anticorrelated pattern [67]. Interestingly, the oscillating ratios peak at different relative phases for the higher and lower laser intensities. This can be qualitatively understood as following. As shown in Fig. 3(a), the recollision energy reaches its maximum at $\Delta\phi = 0.4\pi$ (1.4π). At this phase, there is also another bunch of events with a much lower recollision energy, which would result in the anticorrelated emission. At the relatively high laser intensities, the combination of these two bunches of events makes the correlated emission is less prevalent at $\Delta\phi = 0.4\pi$ (1.4π) than $\Delta\phi = 0.25\pi$ (1.25π) where the lower-energy bunch disappears. At the lower laser intensity, the recollision energy is very low and thus only when the recollision energy reach its maximum at the $\Delta\phi = 0.4\pi$ (1.4π) could result in dominantly correlated emission. Consequently, the ratio peaks at $\Delta\phi = 0.4\pi$ (1.4π).

4. Conclusion

In conclusion, we have theoretically studied the correlated electron dynamics in the linearly polarized two-color laser fields. Our results show that the scheme of two-color field is an efficient tool to control the subcycle dynamics of the correlated electrons in strong-field NSDI, more specifically, the decay dynamics of recollision-induced excited states in NSDI. The control of the recollision time and correspondingly the recollision energy results in the single- and double-hump structures in the ion momentum distributions. The single-hump structure indicates that NSDI is dominated by the RESI way with time delay longer than a quarter laser cycle. In the double-hump structure, the peak located at zero and nonzero momenta correspond to the NSDI events where the time delay is larger and less than a quarter laser cycle, respectively. Thus, the electron dynamics for each peaks in the measurable ion momentum spectra can be determined.

Funding

National Natural Science Foundation of China (NNSFC) (11622431, 61405064 and 11234004).

Acknowledgments

Numerical simulations presented in this paper were carried out using the High Performance Computing Center experimental testbed in SCTS/CGCL (see http://grid.hust.edu.cn/hpcc).

Appendix A. Supplementary material

Supplementary data associated with this article can be found, in the online version, at https://doi.org/10.1016/j.optlastec.2018.06.058.

References

[1] K.J. Schafer, B. Yang, L.F. DiMauro, K.C. Kulander, Above threshold ionization beyond the high harmonic cutoff, Phys. Rev. Lett. 70 (11) (1993) 1599–1602, https://doi.org/10.1103/PhysRevLett.70.1599.

[2] P.B. Corkum, Plasma perspective on strong field multiphoton ionization, Phys. Rev. Lett. 71 (13) (1993) 1994–1997, https://doi.org/10.1103/PhysRevLett.71.1994.

[3] F. Krausz, M. Ivanov, Attosecond physics, Rev. Mod. Phys. 81 (1) (2009) 163–234, https://doi.org/10.1103/RevModPhys.81.163.

[4] C. Zhai, X. Zhang, X. Zhu, L. He, Y. Zhang, B. Wang, Q. Zhang, P. Lan, P. Lu, Single-shot molecular orbital tomography with orthogonal two-color fields, Opt. Express 26 (3) (2018) 2775–2784, https://doi.org/10.1364/OE.26.002775.

[5] L. He, Q. Zhang, P. Lan, W. Cao, X. Zhu, C. Zhai, F. Wang, W. Shi, M. Li, X.B. Bian, P. Lu, A.D. Bandrauk, Monitoring ultrafast vibrational dynamics of isotopic molecules with frequency modulation of high-order harmonics, Nat. Commun. 9 (1) (2018) 1108, https://doi.org/10.1038/s41467-018-03568-3.

[6] W. Becker, F. Grasbon, R. Kopold, D.B. Milosevic, G.G. Paulus, H. Walther, Above-threshold ionization: from classical features to quantum effects, Adv. Atomic Mol. Opt. Phys. 48 (1979) (2002) 35–98, https://doi.org/10.1016/S1049-250X(02)80006-4.

[7] Y. Zhou, O.I. Tolstikhin, T. Morishita, Near-forward rescattering photoelectron holography in strong-field ionization: extraction of the phase of the scattering amplitude, Phys. Rev. Lett. 116 (17) (2016) 173001, https://doi.org/10.1103/PhysRevLett.116.173001.

[8] Z. Wang, M. Li, Y. Zhou, P. Lan, P. Lu, Correlated electron-nuclear dynamics in above-threshold multiphoton ionization of asymmetric molecule, Sci. Rep. 7 (2016) (2017) 42585, https://doi.org/10.1038/srep42585.

[9] M. He, Y. Zhou, Y. Li, M. Li, P. Lu, Revealing the target structure information encoded in strong-field photoelectron hologram, Opt. Quant. Electron. 49 (6) (2017) 232, https://doi.org/10.1007/s11082-017-1060-1.

[10] M. He, Y. Li, Y. Zhou, M. Li, W. Cao, P. Lu, Direct visualization of valence electron motion using strong-field photoelectron holography, Phys. Rev. Lett. 120 (13) (2018) 133204, https://doi.org/10.1103/PhysRevLett.120.133204.

[11] A. L'Huillier, L.A. Lompre, G. Mainfray, C. Manus, Multiply charged ions induced by multiphoton absorption in rare gases at 0.53 μm, Phys. Rev. A 27 (5) (1983) 2503–2512, https://doi.org/10.1103/PhysRevA.27.2503.

[12] D.N. Fittinghoff, P.R. Bolton, B. Chang, K.C. Kulander, Observation of nonsequential double ionization of helium with optical tunneling, Phys. Rev. Lett. 69 (18) (1992) 2642–2645, https://doi.org/10.1103/PhysRevLett.69.2642.

[13] B. Walker, B. Sheehy, L.F. DiMauro, P. Agostini, K.J. Schafer, K.C. Kulander, Precision measurement of strong field double ionization of helium, Phys. Rev. Lett. 73 (9) (1994) 1227–1230, https://doi.org/10.1103/PhysRevLett.73.1227.

[14] E. Eremina, X. Liu, H. Rottke, W. Sandner, A. Dreischuh, F. Lindner, F. Grasbon, G.G. Paulus, H. Walther, R. Moshammer, B. Feuerstein, J. Ullrich, Laser-induced non-sequential double ionization investigated at and below the threshold for electron impact ionization, J. Phys. B: At. Mol. Opt. Phys. 36 (15) (2003) 3269–3280, https://doi.org/10.1088/0953-4075/36/15/308.

[15] T. Weber, H. Giessen, M. Weckenbrock, G. Urbasch, A. Staudte, L. Spielberger, O. Jagutzki, V. Mergel, M. Vollmer, R. Dörner, Correlated electron emission in multiphoton double ionization, Nature 405 (6787) (2000) 658–661, https://doi.org/10.1038/35015033.

[16] R. Moshammer, B. Feuerstein, W. Schmitt, A. Dorn, C.D. Schröter, J. Ullrich, H. Rottke, C. Trump, M. Wittmann, G. Korn, K. Hoffmann, W. Sandner, Momentum distributions of Ne^{n+} Ions Created by an Intense ultrashort laser pulse, Phys. Rev. Lett. 84 (3) (2000) 447–450, https://doi.org/10.1103/PhysRevLett.84.447.

[17] M. Weckenbrock, A. Becker, A. Staudte, S. Kammer, M. Smolarski, V.R. Bhardwaj, D.M. Rayner, D.M. Villeneuve, P.B. Corkum, R. Dörner, Electron-electron momentum exchange in strong field double ionization, Phys. Rev. Lett. 91 (12) (2003) 123004, https://doi.org/10.1103/PhysRevLett.91.123004.

[18] D. Zeidler, A. Staudte, A.B. Bardon, D.M. Villeneuve, R. Dörner, P.B. Corkum, Controlling attosecond double ionization dynamics via molecular alignment, Phys. Rev. Lett. 95 (20) (2005) 203003, https://doi.org/10.1103/PhysRevLett.95.203003.

[19] A. Rudenko, T. Ergler, K. Zrost, B. Feuerstein, V.L.B. de Jesus, C.D. Schröter, R. Moshammer, J. Ullrich, Intensity-dependent transitions between different pathways of strong-field double ionization, Phys. Rev. A 78 (1) (2008) 015403, https://doi.org/10.1103/PhysRevA.78.015403.

[20] Y. Liu, L. Fu, D. Ye, J. Liu, M. Li, C. Wu, Q. Gong, R. Moshammer, J. Ullrich, Strong-field double ionization through sequential release from double excitation with subsequent coulomb scattering, Phys. Rev. Lett. 112 (1) (2014) 013003, https://doi.org/10.1103/PhysRevLett.112.013003.

[21] M. Lein, E.K.U. Gross, V. Engel, Intense-field double ionization of helium: identifying the mechanism, Phys. Rev. Lett. 85 (22) (2000) 4707–4710, https://doi.org/10.1103/PhysRevLett.85.4707.

[22] J.S. Parker, B.J.S. Doherty, K.T. Taylor, K.D. Schultz, C.I. Blaga, L.F. DiMauro, High-energy cutoff in the spectrum of strong-field nonsequential double

ionization, Phys. Rev. Lett. 96 (13) (2006) 133001, https://doi.org/10.1103/PhysRevLett.96.133001.

[23] J.S. Prauzner-Bechcicki, K. Sacha, B. Eckhardt, J. Zakrzewski, Time-resolved quantum dynamics of double ionization in strong laser fields, Phys. Rev. Lett. 98 (20) (2007) 203002, https://doi.org/10.1103/PhysRevLett.98.203002.

[24] D.I. Bondar, G.L. Yudin, W.-K. Liu, M.Y. Ivanov, A.D. Bandrauk, Nonsequential double ionization below laser-intensity threshold: anticorrelation of electrons without excitation of parent ion, Phys. Rev. A 83 (1) (2011) 013420, https://doi.org/10.1103/PhysRevA.83.013420.

[25] C. Figueira de Morisson Faria, H. Schomerus, X. Liu, W. Becker, Electron-electron dynamics in laser-induced nonsequential double ionization, Phys. Rev. A 69 (4) (2004) 043405, https://doi.org/10.1103/PhysRevA.69.043405.

[26] X. Hao, J. Chen, W. Li, B. Wang, X. Wang, W. Becker, Quantum effects in double ionization of argon below the threshold intensity, Phys. Rev. Lett. 112 (7) (2014) 073002, https://doi.org/10.1103/PhysRevLett.112.073002.

[27] D.F. Ye, X. Liu, J. Liu, Classical trajectory diagnosis of a fingerlike pattern in the correlated electron momentum distribution in strong field double ionization of helium, Phys. Rev. Lett. 101 (23) (2008) 233003, https://doi.org/10.1103/PhysRevLett.101.233003.

[28] K. Sacha, B. Eckhardt, Pathways to double ionization of atoms in strong fields, Phys. Rev. A 63 (4) (2001) 043414, https://doi.org/10.1103/PhysRevA.63.043414.

[29] R. Panfili, S.L. Haan, J.H. Eberly, Slow-down collisions and nonsequential double ionization in classical simulations, Phys. Rev. Lett. 89 (11) (2002) 113001, https://doi.org/10.1103/PhysRevLett.89.113001.

[30] Y. Zhou, Q. Liao, P. Lu, Mechanism for high-energy electrons in nonsequential double ionization below the recollision-excitation threshold, Phys. Rev. A 80 (2) (2009) 023412, https://doi.org/10.1103/PhysRevA.80.023412.

[31] F. Mauger, C. Chandre, T. Uzer, Recollisions and correlated double ionization with circularly polarized light, Phys. Rev. Lett. 105 (8) (2010) 083002, https://doi.org/10.1103/PhysRevLett.105.083002.

[32] Y. Chen, Y. Zhou, Y. Li, M. Li, P. Lan, P. Lu, Rabi oscillation in few-photon double ionization through doubly excited states, Phys. Rev. A 97 (1) (2018) 013428, https://doi.org/10.1103/PhysRevA.97.013428.

[33] B. Feuerstein, R. Moshammer, D. Fischer, A. Dorn, C.D. Schröter, J. Deipenwisch, J.R. Crespo Lopez-Urrutia, C. Höhr, P. Neumayer, J. Ullrich, H. Rottke, C. Trump, M. Wittmann, G. Korn, W. Sandner, Separation of recollision mechanisms in nonsequential strong field double ionization of Ar: the role of excitation tunneling, Phys. Rev. Lett. 87 (4) (2001) 043003, https://doi.org/10.1103/PhysRevLett.87.043003.

[34] D. Ye, M. Li, L. Fu, J. Liu, Q. Gong, Y. Liu, J. Ullrich, Scaling laws of the two-electron sum-energy spectrum in strong-field double ionization, Phys. Rev. Lett. 115 (12) (2015) 123001, https://doi.org/10.1103/PhysRevLett.115.123001.

[35] X. Ma, Y. Zhou, P. Lu, Multiple recollisions in strong-field nonsequential double ionization, Phys. Rev. A 93 (1) (2016) 013425, https://doi.org/10.1103/PhysRevA.93.013425.

[36] C. Huang, M. Zhong, Z. Wu, Recollision dynamics in nonsequential double ionization of atoms by long-wavelength pulses, Opt. Express 24 (25) (2016) 28361–28371, https://doi.org/10.1364/OE.24.028361.

[37] Y.-B. Li, X. Wang, B.-H. Yu, Q.-B. Tang, G.-H. Wang, J.-G. Wan, Nonsequential double ionization with mid-infrared laser fields, Sci. Rep. 6 (1) (2016) 37413, https://doi.org/10.1038/srep37413.

[38] X. Ma, M. Li, Y. Zhou, P. Lu, Nonsequential double ionization of Xe by mid-infrared laser pulses, Opt. Quant. Electron. 49 (4) (2017) 170, https://doi.org/10.1007/s11082-017-1002-y.

[39] A. Baltuška, T. Udem, M. Uiberacker, M. Hentschel, E. Goulielmakis, C. Gohle, R. Holzwarth, V.S. Yakovlev, A. Scrinzi, T.W. Hänsch, F. Krausz, Attosecond control of electronic processes by intense light fields, Nature 421 (6923) (2003) 611–615, https://doi.org/10.1038/nature01414.

[40] X. Liu, H. Rottke, E. Eremina, W. Sandner, E. Goulielmakis, K.O. Keeffe, M. Lezius, F. Krausz, F. Lindner, M.G. Schätzel, G.G. Paulus, H. Walther, Nonsequential double ionization at the single-optical-cycle limit, Phys. Rev. Lett. 93 (26) (2004) 263001, https://doi.org/10.1103/PhysRevLett.93.263001.

[41] B. Bergues, M. Kübel, N.G. Johnson, B. Fischer, N. Camus, K.J. Betsch, O. Herrwerth, A. Senftleben, A.M. Sayler, T. Rathje, T. Pfeifer, I. Ben-Itzhak, R.R. Jones, G.G. Paulus, F. Krausz, R. Moshammer, J. Ullrich, M.F. Kling, Attosecond tracing of correlated electron-emission in non-sequential double ionization, Nat. Commun. 3 (3) (2012) 813, https://doi.org/10.1038/ncomms1807.

[42] M. Kübel, K.J. Betsch, N.G. Kling, A.S. Alnaser, J. Schmidt, U. Kleineberg, Y. Deng, I. Ben-Itzhak, G.G. Paulus, T. Pfeifer, J. Ullrich, R. Moshammer, M.F. Kling, B. Bergues, Non-sequential double ionization of Ar: from the single- to the many-cycle regime, New J. Phys. 16 (3) (2014) 033008, https://doi.org/10.1088/1367-2630/16/3/033008.

[43] Y. Chen, Y. Zhou, Y. Li, M. Li, P. Lan, P. Lu, The contribution of the delayed ionization in strong-field nonsequential double ionization, J. Chem. Phys. 144 (2) (2016) 024304, https://doi.org/10.1063/1.4939642.

[44] N. Camus, B. Fischer, M. Kremer, V. Sharma, A. Rudenko, B. Bergues, M. Kübel, N.G. Johnson, M.F. Kling, T. Pfeifer, J. Ullrich, R. Moshammer, Attosecond correlated dynamics of two electrons passing through a transition state, Phys. Rev. Lett. 108 (7) (2012) 073003, https://doi.org/10.1103/PhysRevLett.108.073003.

[45] M. Kübel, N.G. Kling, K.J. Betsch, N. Camus, A. Kaldun, U. Kleineberg, I. Ben-Itzhak, R.R. Jones, G.G. Paulus, T. Pfeifer, J. Ullrich, R. Moshammer, M.F. Kling, B. Bergues, Nonsequential double ionization of N_2 in a near-single-cycle laser pulse, Phys. Rev. A 88 (2) (2013) 023418, https://doi.org/10.1103/PhysRevA.88.023418.

[46] K. Lin, X. Jia, Z. Yu, F. He, J. Ma, H. Li, X. Gong, Q. Song, Q. Ji, W. Zhang, H. Li, P. Lu, H. Zeng, J. Chen, J. Wu, Comparison study of strong-field ionization of molecules and atoms by bicircular two-color femtosecond laser pulses, Phys. Rev. Lett. 119 (20) (2017) 203202, https://doi.org/10.1103/PhysRevLett.119.203202.

[47] Q. Song, P. Lu, X. Gong, Q. Ji, K. Lin, W. Zhang, J. Ma, H. Zeng, J. Wu, Dissociative double ionization of co in orthogonal two-color laser fields, Phys. Rev. A 95 (1) (2017) 013406, https://doi.org/10.1103/PhysRevA.95.013406.

[48] E.J. Takahashi, P. Lan, O.D. Mücke, Y. Nabekawa, K. Midorikawa, Infrared two-color multicycle laser field synthesis for generating an intense attosecond pulse, Phys. Rev. Lett. 104 (23) (2010) 233901, https://doi.org/10.1103/PhysRevLett.104.233901.

[49] J. Tan, Y. Li, Y. Zhou, M. He, Y. Chen, M. Li, P. Lu, Identifying the contributions of multiple-returning recollision orbits in strong-field above-threshold ionization, Opt. Quant. Electron. 50 (2) (2018) 57, https://doi.org/10.1007/s11082-018-1332-4.

[50] L. Zhang, X. Xie, S. Roither, Y. Zhou, P. Lu, D. Kartashov, M. Schöffler, D. Shafir, P. B. Corkum, A. Baltuška, A. Staudte, M. Kitzler, Subcycle control of electron-electron correlation in double ionization, Phys. Rev. Lett. 112 (19) (2014) 193002, https://doi.org/10.1103/PhysRevLett.112.193002.

[51] Y. Zhou, C. Huang, A. Tong, Q. Liao, P. Lu, Correlated electron dynamics in nonsequential double ionization by orthogonal two-color laser pulses, Opt. Express 19 (3) (2011) 2301–2308, https://doi.org/10.1364/OE.19.002301.

[52] C.A. Mancuso, K.M. Dorney, D.D. Hickstein, J.L. Chaloupka, J.L. Ellis, F.J. Dollar, R. Knut, P. Grychtol, D. Zusin, C. Gentry, M. Gopalakrishnan, H.C. Kapteyn, M.M. Murnane, Controlling nonsequential double ionization in two-color circularly polarized femtosecond laser fields, Phys. Rev. Lett. 117 (13) (2016) 133201, https://doi.org/10.1103/PhysRevLett.117.133201.

[53] S. Eckart, M. Richter, M. Kunitski, A. Hartung, J. Rist, K. Henrichs, N. Schlott, H. Kang, T. Bauer, H. Sann, L.P.H. Schmidt, M. Schöffler, T. Jahnke, R. Dörner, Nonsequential double ionization by counterrotating circularly polarized two-color laser fields, Phys. Rev. Lett. 117 (13) (2016) 133202, https://doi.org/10.1103/PhysRevLett.117.133202.

[54] S.X. Hu, Boosting photoabsorption by attosecond control of electron correlation, Phys. Rev. Lett. 111 (12) (2013) 123003, https://doi.org/10.1103/PhysRevLett.111.123003.

[55] A. Liu, U. Thumm, Laser-assisted XUV few-photon double ionization of helium: joint angular distributions, Phys. Rev. A 89 (6) (2014) 063423, https://doi.org/10.1103/PhysRevA.89.063423.

[56] S.L. Haan, J.S. Van Dyke, Z.S. Smith, Recollision excitation, electron correlation, and the production of high-momentum electrons in double ionization, Phys. Rev. Lett. 101 (11) (2008) 113001, https://doi.org/10.1103/PhysRevLett.101.113001.

[57] Y. Zhou, Q. Liao, P. Lu, Asymmetric electron energy sharing in strong-field double ionization of helium, Phys. Rev. A 82 (5) (2010) 053402, https://doi.org/10.1103/PhysRevA.82.053402.

[58] C. Huang, Y. Zhou, Q. Zhang, P. Lu, Contribution of recollision ionization to the cross-shaped structure in nonsequential double ionization, Opt. Express 21 (9) (2013) 11382–11390, https://doi.org/10.1364/OE.21.011382.

[59] S.L. Haan, Z.S. Smith, K.N. Shomsky, P.W. Plantinga, Anticorrelated electrons from weak recollisions in nonsequential double ionization, J. Phys. B: At. Mol. Opt. Phys. 41 (21) (2008) 211002, https://doi.org/10.1088/0953-4075/41/21/211002.

[60] X. Wang, J.H. Eberly, Effects of elliptical polarization on strong-field short-pulse double ionization, Phys. Rev. Lett. 103 (10) (2009) 103007, https://doi.org/10.1103/PhysRevLett.103.103007.

[61] A. Tong, Y. Zhou, P. Lu, Resolving subcycle electron emission in strong-field sequential double ionization, Opt. Express 23 (12) (2015) 15774–15783, https://doi.org/10.1364/OE.23.015774.

[62] P.J. Ho, J.H. Eberly, Different rescattering trajectories related to different total electron momenta in nonsequential double ionization, Opt. Express 11 (22) (2003) 2826–2831, https://doi.org/10.1364/OE.11.002826.

[63] Y. Zhou, M. Li, Y. Li, A. Tong, Q. Li, P. Lu, Dissection of electron correlation in strong-field sequential double ionization using a classical model, Opt. Express 25 (7) (2017) 8450–8458, https://doi.org/10.1364/OE.25.008450.

[64] L.-B. Fu, J. Liu, J. Chen, S.-G. Chen, Classical collisional trajectories as the source of strong-field double ionization of helium in the knee regime, Phys. Rev. A 63 (4) (2001) 043416, https://doi.org/10.1103/PhysRevA.63.043416.

[65] M.V. Ammosov, N.B. Delone, V.P. Krainov, Tunnel ionization of complex atoms and atomic ions in electromagnetic field, in: J.A. Alcock (Ed.), Sov. Phys. JETP, vol. 64, 1986, pp. 1191–1194. https://doi.org/10.1117/12.938695.

[66] C. Huang, W. Guo, Y. Zhou, Z. Wu, Role of Coulomb repulsion in correlated-electron emission from a doubly excited state in nonsequential double ionization of molecules, Phys. Rev. A 93 (1) (2016) 013416, https://doi.org/10.1103/PhysRevA.93.013416.

[67] Y. Liu, S. Tschuch, A. Rudenko, M. Dürr, M. Siegel, U. Morgner, R. Moshammer, J. Ullrich, Strong-field double ionization of Ar below the recollision threshold, Phys. Rev. Lett. 101 (5) (2008) 053001, https://doi.org/10.1103/PhysRevLett.101.053001.